

## **Identification of Potent Inhibitors of Drug-Sensitive and Drug-Resistant Plasmodium Falciparum**

Uday CK\*, Shaik Mahmood

Bioinformatics Division, Environmental Microbiology Lab, Department of Botany, Osmania

University, Hyderabad 500 007, A.P., India

### **Summary**

Malaria is a disease that causes more than 1 million deaths per year worldwide and more than 400 million clinical cases. Due to the acquired resistance of *Plasmodium falciparum* to the drugs used to control the infection, searching for new anti-malaria drugs is necessary in modern days. Recent studies have shown that the parasite synthesizes fatty acids using a fatty acid synthase type II (FAS-II) instead of a type-I fatty acid synthase (FAS-I) that is present in other eukaryotes. *Plasmodium falciparum* enoyl reductase (PfENR) is responsible for the last step of fatty acid biosynthesis in the parasite. This enzyme is located within the apicoplast, a plastid-like organelle that is responsible for several important metabolic pathways, including fatty acid biosynthesis. It is known that triclosan is an inhibitor of ENR in bacteria and we and others have shown that it is also effective against ENR in apicomplexan organisms such as *P. falciparum*. Three dimensional pharmacophore model was developed based on available *P. falciparum* enoyl acyl carrier protein (ACP) reductase inhibitors which were carefully selected with great diversity in both molecular structure and bioactivity as required by Hypo Gen program in the catalyst software in Discovery studio 2.5, Accelrys product for discovering new *Pf* EACP reductase inhibitors. Out of 41 molecules, 18 were taken as training set and remaining 23 were used for test set validation. The common feature pharmacophore or hip-hop consisted of four features namely two hydrogen bond acceptors, one hydrophobic and one hydrophobic aromatic. The best hypothesis of hypogen run consisting of four features namely two hydrogen bond acceptors and two hydrophobic, has a correlation coefficient of 0.958, a root mean square deviation of 1.044 and a cost difference of 93.241, suggesting that a highly predictive pharmacophore model was successfully obtained. The application of the model shows great success in predicting the activities of 23 known *Pf* EACP reductase inhibitors in our test set with a correlation coefficient of 0.752(r). Accordingly, our model should be reliable in identifying structurally diverse compounds with desired biological activity. The next part of the study involved docking of two highly active and two low active *Pf* EACP reductase inhibitors against the *Pf* EACP reductase crystal protein using CDocker docking protocol available in Discovery studio2.5. The CDocker energies of two highly active inhibitors were -34.893 and -22.831 while that of one moderately active and one low active inhibitor were -21.447 and -19.847 respectively. All of the above four molecules showed interactions with the receptor mostly at Lys285 and Ser317 residues which are also existing among the crystal ligand interactions. Both from pharmacophore studies and from docking studies the results have shown that Triclosan and 2' substituted Triclosan derivatives were high active inhibitors.

## Introduction

Malaria was found to be one of the most devastating diseases of the tropical countries. Over three billion people live under the threat of malaria across the world and it kills over a million each year, mostly children [1]. The development of novel anti-malarials is critical as malaria worldwide afflicts 300–600 million people resulting in 1–3 million deaths per year [2]. Traditional treatments with drugs, such as chloroquine and sulfadoxine-pyrimethamine, are now much less effective due to rampant resistance [3]. The inhibition of fatty acid synthesis in *P. falciparum* holds significant promise in potentially enabling the discovery and development of an orally dosed therapeutic that is affordable, safe, and efficacious against drug-resistant strains. Fatty acid synthesis plays a key role in membrane construction and energy production [4]. Fatty acid biosynthesis is an iterative process beginning with the condensation of acetyl Co A with the growing fatty acid chain. *P. falciparum* enoyl acyl carrier protein (ACP) reductase is responsible for the final step in each fatty acid synthesis cycle: the NADH dependent reduction of trans-2-enoyl-ACP to acyl-ACP [5]. Triclosans, Rhodanine class of compounds, diphenyl and diaryl ether compounds which are substituted triclosan derivatives and flavonoids were identified from literature as template compounds for inhibitors against *Plasmodium falciparum* enoyl acyl carrier protein reductase [5-9]. The lack of suitable alternatives to replace chloroquine and sulfadoxine, and the limited extent of triclosan usage, threatens efforts to control the rapid spread of drug resistant strains of this parasite, and adds to the need for pharmaceutical discoveries to overcome existing barriers [10]. Recently, the X-ray crystal structure of *P. falciparum* enoyl acyl carrier protein (ACP) reductase was determined in complex with triclosan [11]. A widely used antibiotic, triclosan is a potent inhibitor of *P. falciparum* enoyl acyl carrier protein (ACP) reductase enzyme activity and *Plasmodium* growth both in vitro and in vivo [12]. Triclosan has been approved for use as a topical antibacterial drug and can be found in many soaps and toothpastes. It has been shown to be effective in reducing and controlling bacterial contamination on the hands and on treated products. However, triclosan is not orally bio-available. A number of nano-technological approaches were recently evaluated for the development of an oral delivery method capable of systemic release of triclosan [13]. In this study, we present an image of the primary pharmacophore features responsible for the bioactivity of different classes of *P. falciparum* enoyl acyl carrier protein (ACP) reductase inhibitors using the Catalyst software in Discovery studio2.5, with aim to understand the inhibitory mode of various classes of *P. falciparum* enoyl acyl carrier protein (ACP) reductase inhibitors and to discover new anti-malarial drug leads. This also has been confirmed by docking of two highly active and two low active inhibitors against the *P. falciparum* enoyl acyl carrier protein (ACP) reductase protein.

## Materials and methods

A set of 42 different compounds have been collected from different references [5-9, 14, 15, 23] which involves most class of *P. falciparum* enoyl acyl carrier protein (ACP) reductase inhibitors. The datasets are divided into a training set and a test set. We selected 7 highly active inhibitor compounds for running hip-hop which were having both structural and activity diversity. We selected 18 compounds as training set for hypogen with the following rules: A) Both training set and test sets should have structure taken from similar class of compounds and cover the classes as wide as possible to ensure structural diversity. B) Both training and test sets should cover the molecular bioactivities (IC<sub>50</sub>) as wide as possible. C) The most active compounds should be

included because they provide critical information on pharmacophore requirements. The training set consists of 25 compounds with significant structural diversity and wide coverage of molecular bioactivities in terms of  $IC_{50}$  ranging from 0.036 to 1400  $\mu$ M. To validate our pharmacophore hypothesis, 23 compounds with available  $IC_{50}$  values were used as a test set.

The compounds were built using AccelrysDiscoverystudio2.5, [16] and a family of representative conformations was generated for each compound using the best conformational analysis method with Poling algorithm [17] and CHARMM force field parameters [18]. A maximum number of 250 conformations of each compound were selected using 'best conformer generation' option above the minimum conformer searched to ensure maximum coverage of the conformational space. The crystal structure of *P. falciparum* enoyl acyl carrier protein (ACP) reductase produced from *E. coli* expression system (PDB code: 2NQ8) was obtained from PDB database ([www.rcsb.org](http://www.rcsb.org)) [19]. Structure based drug design was also carried out here by a docking method called CDocker.

*Pharmacophore generation:* Based on the conformations for each compound, Catalyst package in Discoverystudio2.5 was employed to construct possible pharmacophore models [20].

Hypothesis generation in Catalyst at hip-hop mode has one step called constructive phase. In AccelrysDiscoverystudio2.5, hip-hop is run by using a protocol called "Common feature pharmacophore Generation" which is listed under a cluster of protocols related to pharmacophore. All various conformations for highly active six molecule training set was given as input for ligands, 10 pharmacophore features were given as maximum features input and any four features were considered as minimum number. All the other parameters are set accordingly in this protocol. The dataset was also added with Principal value of 2 and Maximum omitted features as 0 for two most highly active molecules and both as value of 1 to all the remaining molecules. The ten features taken in hip-hop were H-bond donor, H-bond acceptor, hydrophobic, hydrophobic aromatic, hydrophobic aliphatic, positive-charge, positive-ionizable, negative-charge, negative-ionizable and ring aromatic. Hypothesis generation in Catalyst at hypogen mode has three steps, which is constructive phase, subtractive phase, and optimization phase, respectively. In AccelrysDiscoverystudio2.5, hypogen is run by using a protocol called "3D QSAR Pharmacophore Generation" which is also listed under pharmacophore protocol cluster. The main inputs to run this protocol were various conformations for training set (18 molecules) and the common features that result from hip-hop. Also the minimum number of features was set as 4 and maximum as 5. All the other parameters were set accordingly. Catalyst identifies actives in constructive phase, while it identifies inactives in subtractive phase. Then in optimization phase, Catalyst attempts to minimize a cost function consisting of two terms. One penalizes the deviation between the estimated activities of the training set molecules and their experimental values; the other penalizes the complexity of the hypothesis. The generation process stops when the optimization no longer improves the score. Uncertainty influences the first step, called the constructive phase, in the hypothesis generating process [21]. The uncertainty value of 2 was used for the compound activity, representing the ratio of the uncertainty range of measured biological activity against the actual activity for each compound. The hypogen results were validated internally by cost difference, RMS deviation, correlation coefficient and configurational cost. It was externally validated by various conformations generated for a 23 molecule test set. This was done by using a protocol called "Ligand pharmacophore Mapping" also listed under pharmacophore protocol cluster. Common feature pharmacophore analysis revealed that three chemical features, viz., hydrogen-bond acceptors (HA), hydrophobic group (HY), and hydrophobic aromatic group (HA), could effectively map all of the critical chemical

features. Hence, the three features were selected to form the essential information in this hypothesis generation process. Analysis of results of hypogen and ligand pharmacophore mapping is done in results section.

*Docking:* The docking method that is used in this study is CDOCKER [22]. To perform docking process with the crystal protein 2NQ8 a protocol called “Dockligands (CDOCKER)” is selected among those listed under receptor-ligand interactions protocol cluster. The receptor protein is prepared by deleting B, C and D chains, water molecules and B heteroatom from the protein hierarchy and only A chain and its crystal ligand (A heteroatom) are retained. Then hydrogens are added to it and by keeping fixed atom constraints (Tool panel → simulate structures → constraints → create fixed atom constraint) on side chain and backbone of the receptor molecule, only the hydrogens are minimized. The force field applied is charmM to the receptor and the hydrogens are minimized. After minimization the constraints are removed. The protein is split into the protein part and crystal ligand part. By selecting only the protein part and by clicking on “define selected molecule as receptor” under define and edit binding site sub panel of the Tool panel the protein is defined as receptor molecule. By selecting only the ligand part and clicking on “Define sphere from selection” so that the copied ligand from one of the templates into the model is used to define the binding site of 15 Angstroms on the receptor molecule. Now the above prepared receptor is given as input for ‘input receptor molecule’ parameter in the LigandFit protocol parameter explorer. Four inhibitors (two high active and two lowactive) of *P. falciparum* enoyl acyl carrier protein (ACP) reductase are taken from the existing molecules that could establish them as *P. falciparum* enoyl acyl carrier protein (ACP) reductase inhibitors. These are sketched in separate windows and saved. Force fields are applied on the molecules and minimized to get lowest energy minimum structure. Each of them is given as input in another parameter meant for ‘input ligands’ and the protocol was run as many times as the number of inhibitors is selected for the experiment. The various conformations for ligand in this procedure were generated by using molecular dynamics. The generated initial structures for the ligand are further refined using simulated annealing. The CDOCKER energy (-(protein-ligand interaction energies)) of best poses docked into the receptor of all the 4 inhibitors ( compounds 3, 8, 14 and 18) is calculated and compared with that of interacting residues at active site region with the crystallized inhibitor in caspase5 modeled protein copied from the template.

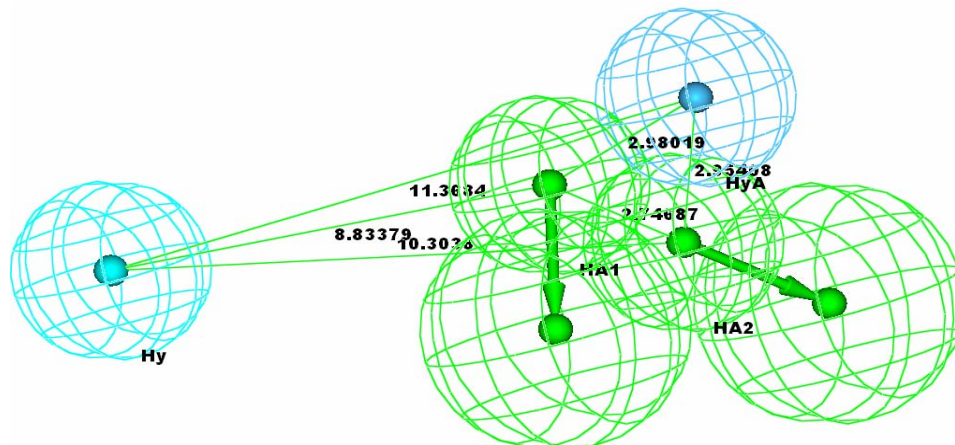
### Results and Discussion

*Hip-hop mode:* Important common pharmacophore features were computed by HipHop encoded in Catalyst embedded in Accelrys Discovery studio2.5. The common pharmacophoric features were obtained as top 10 hypotheses (**Table 1**). The fit values of all the 7 training set molecules were ranging from 3.99 to 1.22 of highly mapped molecule to molecule showing low mapping. The 3D arrangement of features and the mapping of high and low active molecules on hip-hop generated best pharmacophore is shown in **Fig. 1**.

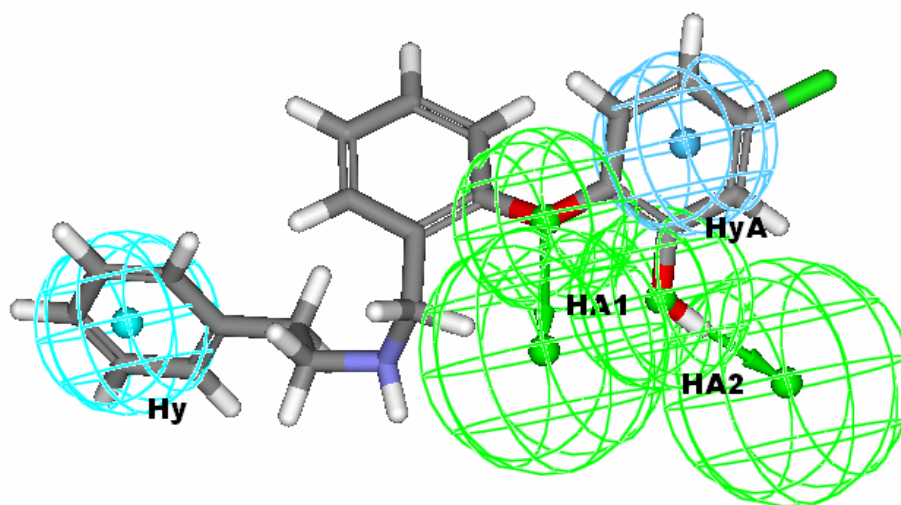
**Table1:** Features shared by top 10 hypotheses in common feature pharmacophore generation

Features	YHA A	RHA A	YHA A	YHA A	RHA A	YHA A	RHA A	YYA A	YYA A	RYA A
Rank	66.81	66.39	65.94	65.43	65.18	64.94	64.70	64.53	64.45	64.41
Hypothesis	1	2	3	4	5	6	7	8	9	10

*Hypogen mode:* Pharmacophores were computed by HypoGen encoded in Catalyst embedded in AccelrysDiscoverystudio2.5 and top 10 hypotheses (**Table 2**) were exported finally. Most hypotheses have high correlation (>0.9). Among all hypotheses four share four features as two hydrogen-bond acceptors, one hydrophobic point, and one hydrophobic aromatic feature, while 2 share four features as two hydrogen-bond acceptors, two hydrophobic points (Hyp01; **Fig. 2**), 2 hypothesis share them as three hydrogen-bond acceptors, one hydrophobic point, and remaining 2 share the features as two hydrogen-bond acceptors, two hydrophobic aromatic.

**Figure1.** a) Best pharmacophore generated by Hiphop (common feature pharmacophore)

b) High active molecule mapping the common feature pharmacophore.



On the basis of the very similar composition of the 10 hypotheses, hypothesis 1 (Hypo1), characterized by the best statistical parameters (**Table 2**) in terms of its predictive ability, as indicated by the highest correlation coefficient and lowest RMS deviations, has been chosen to represent ‘the pharmacophore model’. Remarkably, the three highest active compounds (compounds 1, 2, and 3 in **Table 3**) can be nicely mapped onto the Hypo1 model by the best fit values, which are shown in **Figures 3A–C**, indicating that the Hypo1 model provides reasonable pharmacophoric characteristics of the *P.falciparum* enoyl acyl carrier protein (ACP) reductase inhibitors for components of their activities.

*Cost Analysis:* In addition to generating a hypothesis, Catalyst also provides two theoretical costs (represented in bit units) to help assess the validity of the hypothesis. The first is the cost of an ideal hypothesis (fixed cost), which represents the simplest model that fits all data perfectly. The second is the cost of the null hypothesis (null cost), which represents the highest cost of a pharmacophore with no features and which estimates activity to be the average of the activity data of the training set molecules. They represent the upper and lower bounds for the hypotheses that are generated. A generated hypothesis with a score that is substantially below that of the null hypothesis is likely to be statistically significant and bears visual inspection. The greater the difference between the cost of the generated hypothesis and the cost of the null hypothesis, the less likely it is that the hypothesis reflects a chance correlation.

**Table 2:** Top 10 hypotheses details of Hypogen (3D-QSAR pharmacophore generation)

Hypothesis	Total cost	Cost difference <sup>a</sup>	RMS <sup>b</sup>	Correlation (r)	Features <sup>c</sup>	Maximum Fit value
1	76.481	93.241	1.0444	0.958	HA HA Hy Hy	10.3858
2	76.616	93.106	1.0839	0.954	HA HA Hy	9.96899

					HyA	
3	77.2548	92.4672	1.1195	0.951	HA HA HyA Hy	9.91835
4	78.7089	91.0131	1.1806	0.945	HAHA HyAHyA	10.0575
5	80.3736	89.3484	1.2968	0.933	HA HA Hy Hy	9.23746
6	84.1647	85.5573	1.4544	0.915	HA HA HyA Hy	9.09888
7	85.1042	84.6178	1.4812	0.912	HA HA HyA Hy	9.37092
8	87.1602	82.5618	1.57	0.9	HAHA HyA HyA	8.87316
9	90.1774	79.5446	1.6817	0.885	HA HA HA Hy	8.17154
10	91.4404	78.2816	1.723	0.878	HA HA HA Hy	8.15469

<sup>a</sup> Cost difference = null cost - total cost. Null cost = 169.722. Fixed cost = 64.7135. Configuration cost = 11.3337. All cost units are in bits. Configuration cost: a fixed cost which depends on the complexity of the hypothesis space being optimized.

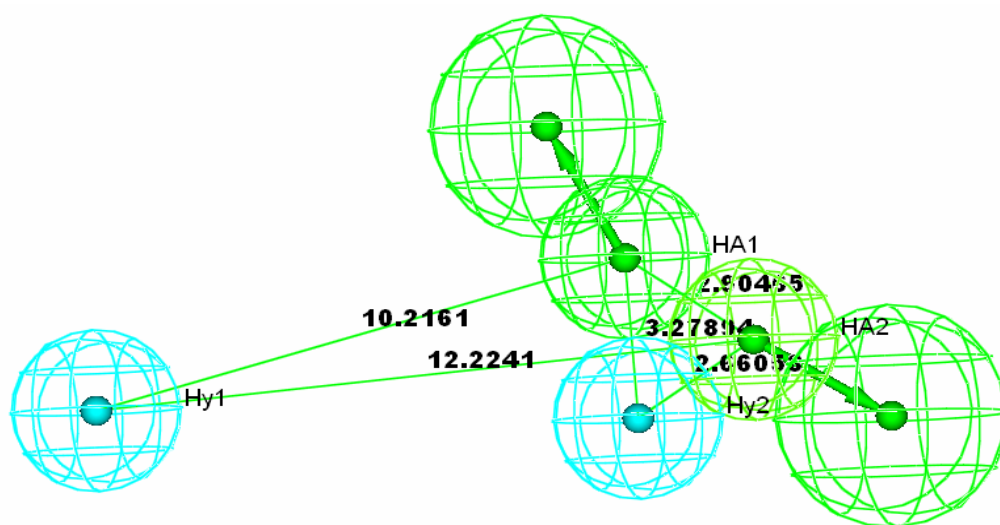
<sup>b</sup> RMS, the deviation of the log (estimated activities) from the log (measured activities) normalized by the log (uncertainties).

<sup>c</sup> HA, hydrogen-bond acceptor; Hy, hydrophobic feature; HyA, hydrophobic aromatic feature

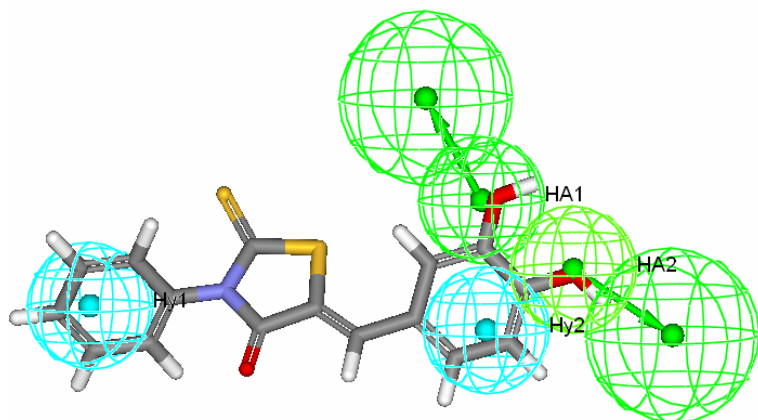
A value of 40–60 bits between them for a pharmacophore hypothesis may indicate that it has 75–90% probability of correlating the data. The total fixed cost of the run is 64.7135, the cost of the null hypothesis is 169.722, and the total cost of the Hypo1 is 76.481 (**Table 2**). Then, the cost range between Hypo1 and the fixed cost is 11.7675, while that between the null hypothesis and Hypo1 is 93.241 (**Table 2**), which shows that Hypo1 has more than 90% probability of correlating the data. Noticeably, the total cost of Hypo1 was much closer to the fixed cost than to the null cost. Furthermore, a high correlation coefficient of 0.958 was observed with RMS value of 1.044 and the configuration cost of 11.3337, demonstrating that we have successfully developed a reliable pharmacophore model with high predictivity.

*Score hypothesis:* To verify Hypo1's discriminability among *P.falciparum* enoyl acyl carrier protein (ACP) reductase inhibitors with different order of magnitude activity, all training set compounds were classified by their activity as highly active (<10 uM, +++), moderately active (10–1000 uM, ++), and inactive (>1000 uM, +). To verify Hypo1's discriminability among *P.falciparum* enoyl acyl carrier protein (ACP) reductase inhibitors with different order of magnitude activity, all training set compounds were classified by their activity as highly active (<10 uM, +++), moderately active (10–1000 uM, ++), and inactive (>1000 uM, +). The actual and estimated *P.falciparum* enoyl acyl carrier protein (ACP) reductase inhibitor activities of the 18 compounds based on Hypo1 are listed in Table 3. The discrepancy between the actual and estimated activity observed for the four compounds was only about 1 order of magnitude, which might be an artifact of the program that uses different number of degrees of freedom for these compounds to mismatch the pharmacophore model. The error factor is also reported in **Table 3**. It shows that all the 18 molecules in the training set have errors less than 10 which means that the activity prediction of these compounds falls between 10-fold greater and 1/10 of the actual activity. The results confirm that our hypothesis is a reliable model for describing the SAR in the training set. In this study, all the 18 molecules could map on hydrophobic2 feature, all except 3 could map on HA1 feature, all except 3 could map on HA2 feature, while 7 molecules could not map on

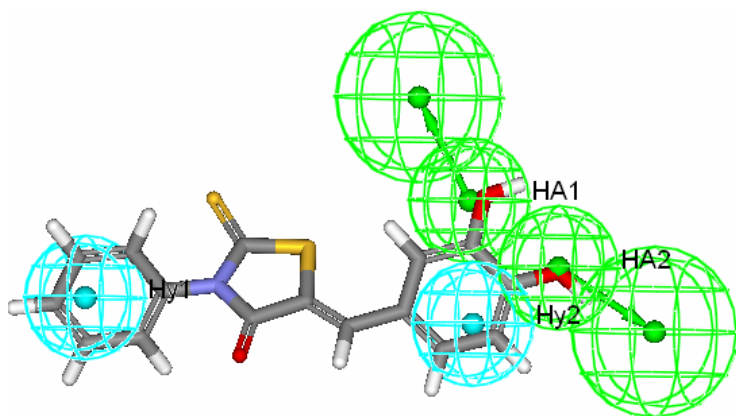
**Figure 2:** Hypo1 (Best pharmacophore) generated by Hypogen (3D QSAR pharmacophore protocol)



A) Compound 1 mapped on Hypo1



B) Compound 2 mapped on Hypo1



C) Compound 3 mapped with Hypo1

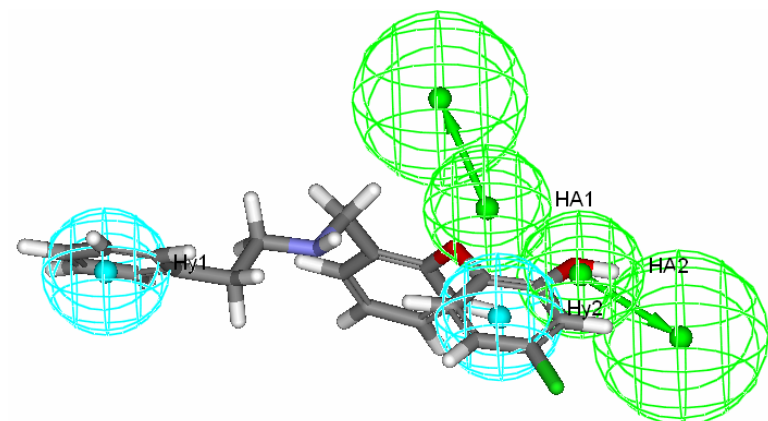


**Figure 3:** First three highest active inhibitors mapped on Hypo1 from the training set.

hydrophobic1 feature (remaining 11 mapped). Only one high active compound was underestimated and activities of all other 17 compounds were estimated as appropriately.

**Table 3:** Details of hypothesis1 (Hypo1)

Compounds	Actual activity ( $\mu\text{M}$ )	Estimated activity ( $\mu\text{M}$ )	Error <sup>a</sup>	Fit-Value <sup>b</sup>	Activity scale <sup>c</sup>	Estimated activity scale	Mapped features		
							HA	HA	Hy
1 (68)	0.035	0.075	2.1	9.794	+++	+++	17	16	22
2 (93)	0.036	0.075	2.1	9.793	+++	+++	14	17	16
3 (67)	2.5	3.885	1.5	8.081	+++	+++	8	9	1
4 (76)	6.5	5.462	3.3	7.933	+++	+++	14	1	13
5 (45)	10	5.512	-1.1	7.929	+++	+++	33	22	7
6 (91)	9	9.579	-1.1	7.689	+++	+++	6	19	1
7 (8)	26	12.705	-2	7.566	++	++	10	8	1
8 (1)	4	12.967	2.9	7.557	+++	++	16	23	-
9 (5)	15	13.584	-1.1	7.537	++	++	4	20	18
10 (90)	19	14.958	-1.2	7.495	++	++	3	16	14
11 (55)	74.59	27.852	-2	7.225	++	++	2	21	19
12 (81)	52	30.754	1.3	7.182	++	++	16	26	8
13 (74)	98.58	31.203	1.2	7.176	++	++	-	23	11
14 (75)	100	32.699	-1.5	7.155	++	++	-	22	8
15 (70)	12.5	36.386	-2.6	7.109	++	++	7	17	21
16 (92)	32	41.093	-3.3	7.056	++	++	21	15	-
17 (80)	50	57.343	-3.1	6.912	++	++	22	20	-
18 (94)	1400	3287.43	2.4	5.153	+	+	-	9	2

<sup>a</sup> The error factor is computed as the ratio of the measured activity to the activity estimated by the hypothesis or the inverse if estimated is greater than measured.

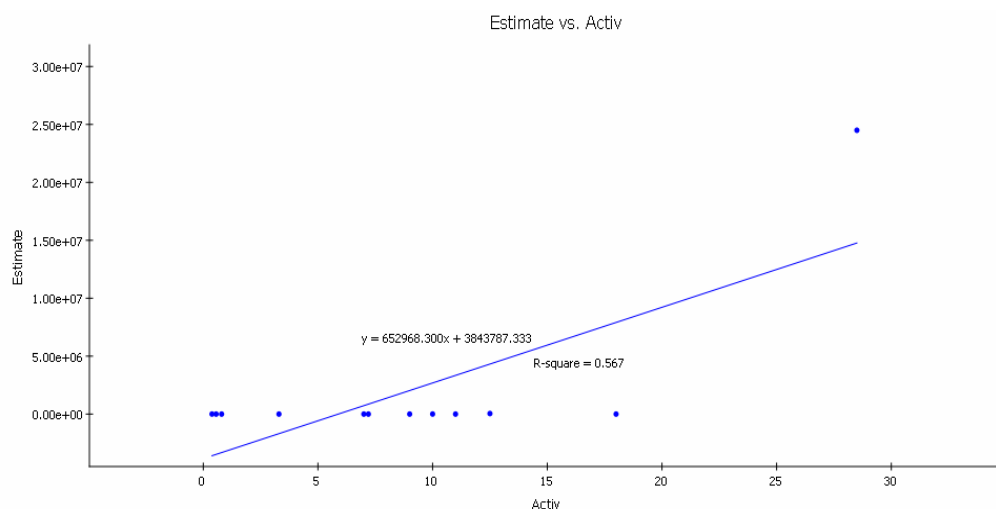
<sup>b</sup> Fit value indicates how well the features in the pharmacophore overlap the chemical features in the molecule.

<sup>c</sup> Activity scale: +++, IC<sub>50</sub> < 10 μM (highly active); ++, 1000 μM > IC<sub>50</sub> > 10 μM (moderately active); +, IC<sub>50</sub>>1000 uM (low active).

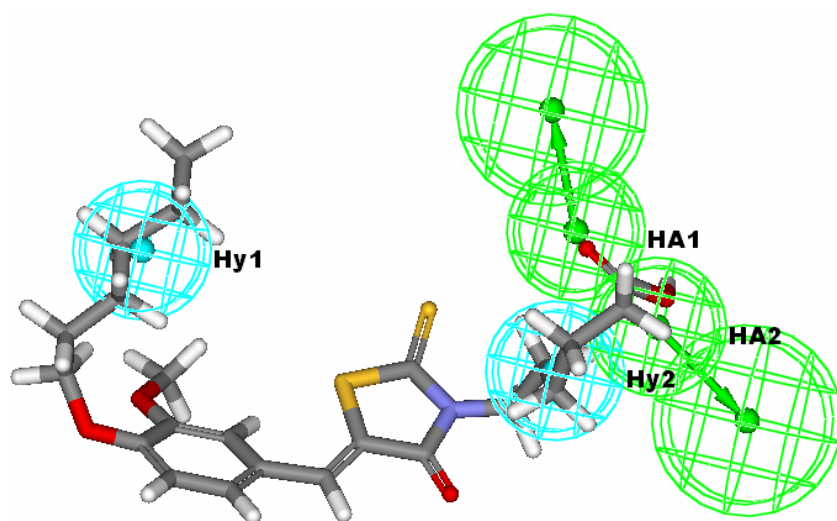
The compounds consisting of 5-Benzylidene-2-thioxothiazolidin-4-one group was proved to be more potent inhibitors according to the previous study [8]. It is also evidently proved by the best pharmacophore here that compound 1, 2 belonging to this group of compounds are mapped to the maximum extent on HA1, HA2, Hy1 and Hy2. The 2'-substituted derivative of Triclosan, compound 3 which is phenethyl analog was found to be most potent against the purified enzyme of *P.falciparum* enoyl ACP reductase [9]. This fact is also evidently proved again in this study by observing its proper mapping on the best pharmacophore.

**Table 4:** Results of ligand pharmacophore mapping of test set (12/23 mapped compounds).

Compound name	Actual activity	Estimated activity	Fit value
19 (77)	7	0.06	9.894
20 (9)	9	0.162	9.46
21 (10)	7.2	0.301	9.192
22 (4)	18	0.891	8.72
23 (89)	11	4.112	8.056
24 (3)	3.3	5.714	7.913
25 (51)	0.56	12.663	7.567
26 (53)	0.8	369.159	6.103
27 (50)	0.38	3802.69	5.09
28 (69)	10	5389.28	4.938
29 (70)	12.5	45655.6	4.011
30 (64)	28.5	2.45E+07	1.281

**Figure 4:** Graphical representation of ligand pharmacophore mapping showing  $r^2$  value.

*Validation of constructed pharmacophore model:* This is done by Ligand pharmacophore mapping. The test set of 23 compounds were taken for mapping purpose. The protocol resulted in successful mapping of 12 compounds on the best pharmacophore (with two HA features and two Hy features). The actual versus estimated activities of 12 compounds is shown in **Table 4**. 4' substituted amide derivatives of triclosan and 5-Benzylidene-2-thioxothiazolidin-4-one class of compounds which are turned out to be compound 19 and 20 were shown to be mapped properly on to the best pharmacophore in this study. They were already proved to be potent inhibitors in the previous studies [5, 8]. The correlation coefficient ( $r$ ) from actual activities against estimated activities of test set was calculated as square root of 0.567 ( $r^2$ ) which is 0.752 [**Fig.4**]. The compound 19 is shown in pharmacophore mapping as high active inhibitor in **Fig.5**.

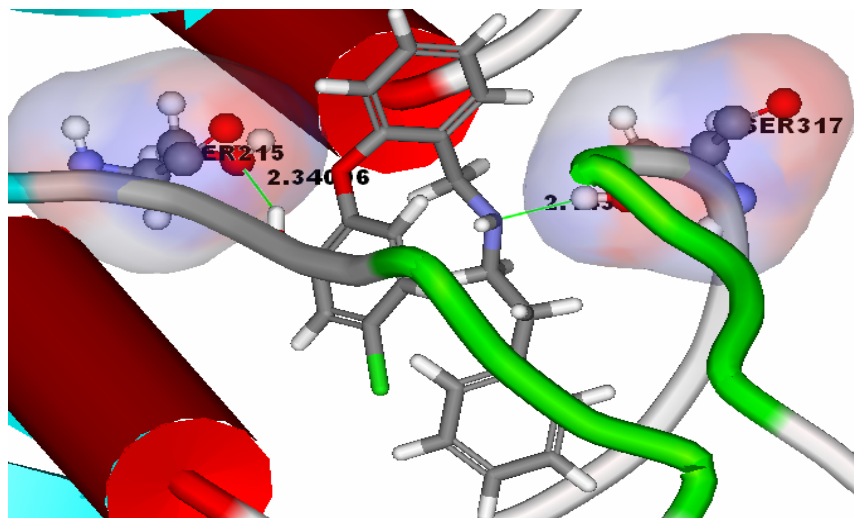
**Figure 5:** High active inhibitor in test set (compound 19) mapped on to Hypo1.

*Docking Analysis:* The crystal protein 2NQ8 taken from PDB database was showing interactions with the crystal ligand at the residues Ser317, Lys285, Ile105, Tyr111 and Leu315. The crystal ligand is isoniazid-NAD adduct which was structurally similar to the lowest active inhibitor of *P.falciparum* enoyl ACP reductase. Four compounds, compound 3 and 8 (experimentally high active), 14 (experimentally moderately active) and 18 (experimentally low active) were docked against the *P.falciparum* enoyl ACP reductase protein. The CDocker energies of two highly active inhibitors were -34.893 and -22.831 while that of one moderately active and one low active inhibitor were -21.447 and -19.847 respectively. All of the above four molecules showed interactions with the receptor mostly at Lys285 and Ser317 residues which are also present among the crystal ligand interactions. The high active molecules showed lower CDocker energies which means that they require less energy for proper interaction with the receptor while the moderately active molecule required more energy than that of high active inhibitors. Low active molecule required still more compared to all others. The docking study has also proved the respective experimental activities of all the four compounds. The details of docking analysis are given in **Table5** and in the **Fig. 6 A-D**.

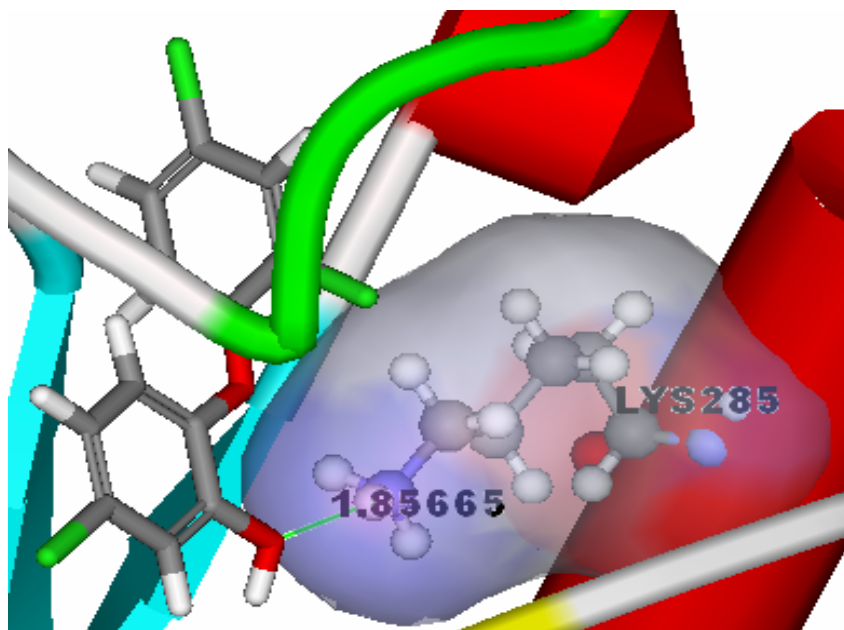
**Table5:** Docking results of four inhibitors of *PfenoylACPreductase*.

Compounds	Activity in $\mu\text{M}$	CDocker energy	Interactions Ligand-Residue	H-bond distance in Angstroms	Interactions
3	2.5	-34.893	H-N...H-O (Ser317)	2.143	Ser317 and Ser215
8	4	-22.831	H-O...H-N (Lys285)	1.856	Lys285
14	100	-21.447	C=S...H-O (Ser317)	2.264	Ser317
18	1400	-19.847	C=O...H-N (Lys285)	2.476	Lys285 and Leu216
			C=O...H-N (Lys285)	1.890	
			H-N...H-N (Lys285)	2.319	

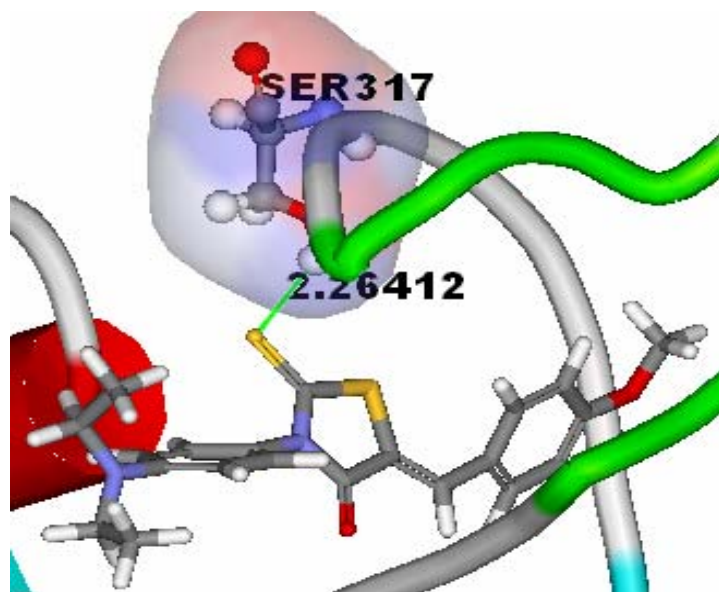
**Figure 6:** The snap shots of docked inhibitors compounds 3, 8, 14 and 18 against *P*fenoylACProductase. A) Compound 3 (highly active) docked into the receptor active site.



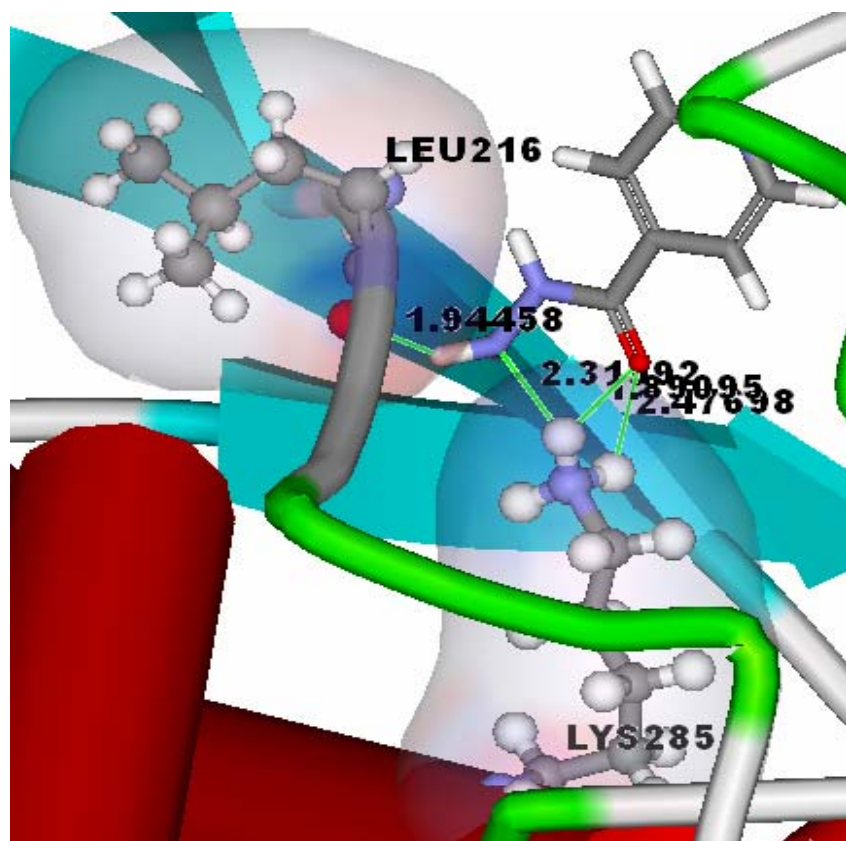
B) Compound 8 (highly active) docked into the receptor active site.



C) Compound 14 (moderately active) docked into the receptor active site.



D) Compound 18 (Low active) docked into the receptor active site.

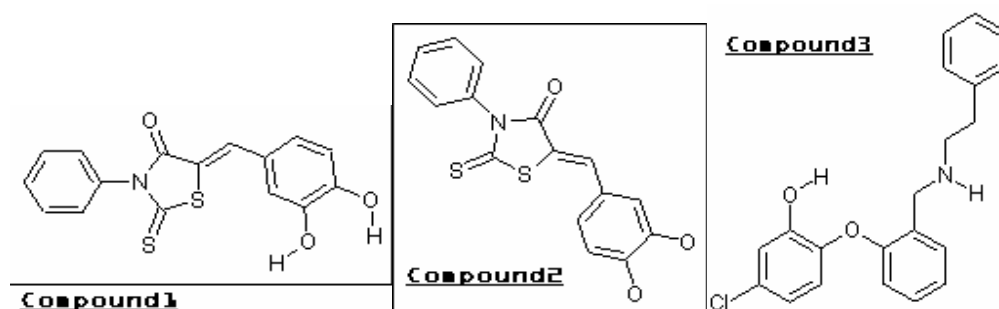


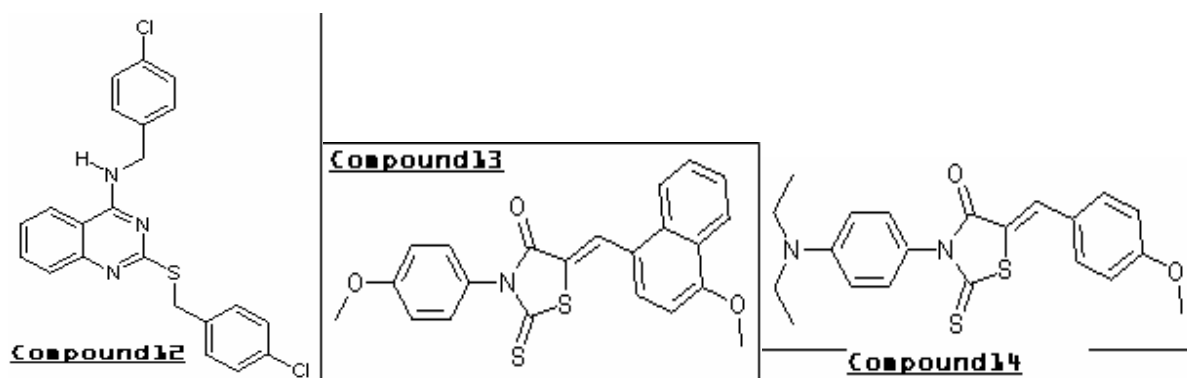
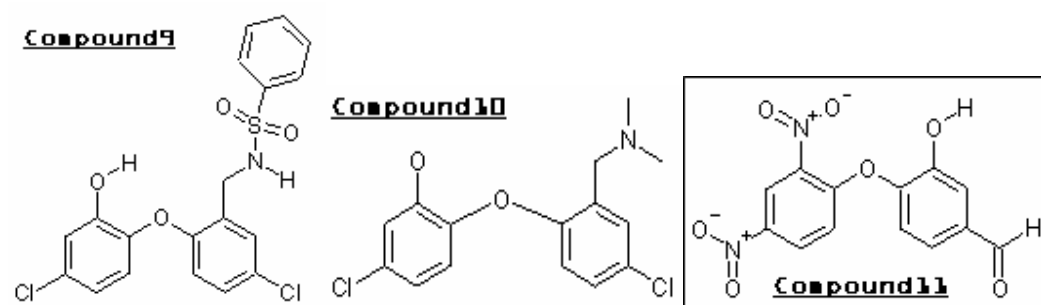
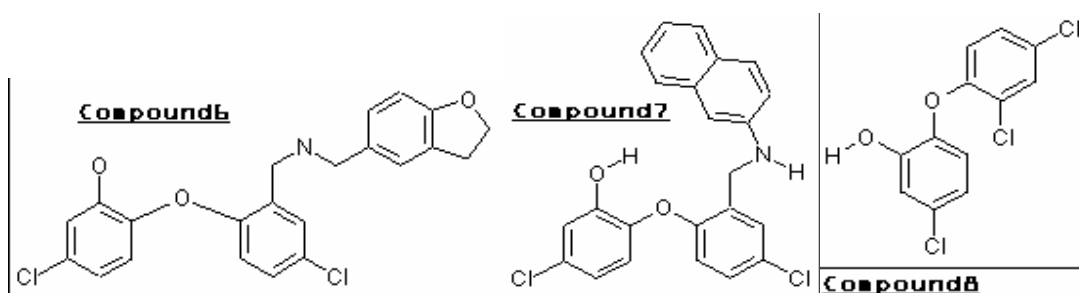
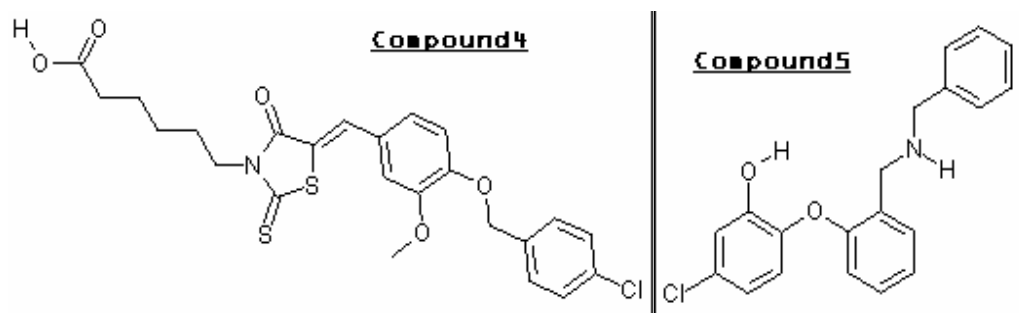
## References

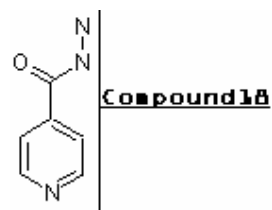
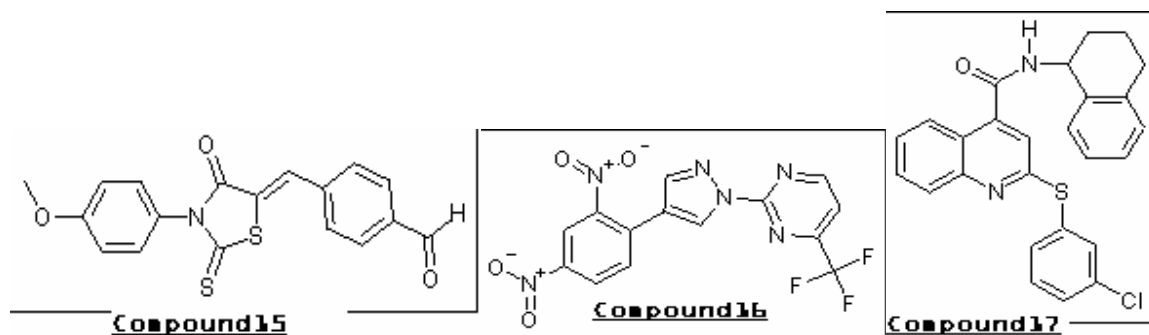
1. WHO World Malaria Report, 2005; World Health Organization: Geneva, Switzerland (<http://rbm.who.int/wmr2005>).
2. Snow, R. W., Guerra, C. A., Noor, A. M., Myint, H. Y., & Hay, S. I. 2005. *Nature*, 434: 214.
3. Greenwood, B., & Mutabingwa, T. 2002. *Nature*, 415:670.
4. Schweizer, E., & Hofmann, J. Microbiol. 2004. *Mol. Biol. Rev.*, 68:501.
5. Joel, S. Freundlich., John, W. Anderson., Dimitri, Sarantakis., Hong-Ming, Shieh., Min, Yu., Juan-Carlos, Valderramos., Edinson, Lucumi., Mack, Kuo., William, R. Jacobs., Jr. David, A. Fidock., Guy, A. Schiehser., David, P. Jacobus., & James, C. Sacchettini. 2005. Synthesis, biological activity, and X-ray crystal structural analysis of diaryl ether inhibitors of malarial enoyl acyl carrier protein reductase. Part 1: 4'-Substituted triclosan derivatives. *Bioorganic & Medicinal Chemistry Letters*, 15:5247–5252
6. Manmohan, Chhibber., Gyanendra, Kumar., Prasanna, Parasuraman., T. N. C. Ramya., Namita, Surolia., & Avadhsha, Surolia. 2006. Novel diphenyl ethers: Design, docking studies, synthesis and inhibition of enoyl ACP reductase of Plasmodium falciparum and Escherichia coli. *Bioorganic & Medicinal Chemistry*, 14: 8086–8098
7. Deniz, Tasdemir., Gabriela, Lack., Reto, Brun., Peter, Ruedi., Leonardo, Scapozz., & Remo, Perozzo.2006. Inhibition of Plasmodium falciparum Fatty Acid Biosynthesis: Evaluation of FabG, FabZ, and FabI as Drug Targets for Flavonoids. *J. Med. Chem.*, 49: 3345-3353
8. Gyanendra, Kumar., Prasann, Parasuraman., Shailendra, Kumar Sharma., Tanushree, Banerjee., Krishanpal, Karmodiya., Namita, Surolia., & Avadhsha, Surolia. 2007. Discovery of a Rhodanine Class of Compounds as Inhibitors of Plasmodium falciparum Enoyl-Acyl Carrier Protein Reductase. *J. Med. Chem.*, 50: 2665-2675.
9. Joel S. Freundlich, John W. Anderson, Dimitri Sarantakis, Hong-Ming Shieh, Min Yu, Juan-Carlos Valderramos, Edinson Lucumi, Mack Kuo, William R. Jacobs, Jr. David A. Fidock, Guy A. Schiehser, David P. Jacobus and James C. Sacchettini. 2006. Synthesis and biological activity of diaryl ether inhibitors of malarial enoyl acyl carrier protein reductase. Part 2: 2'-Substituted triclosan derivatives. *Bioorganic & Medicinal Chemistry Letters*, 16: 2163–2169.
10. Fidock, D. A., Nomura, T., Wellems, T. E. 1998. Cycloguanil and its parent compound proguanil demonstrate distinct activities against Plasmodium falciparum malaria parasites transformed with human dihydrofolate reductase. *Mol Pharmacol.*, 54: 1140–1147.
11. Perozzo, R., Kuo, M., Sidhu, A. S., Valiyaveetil, J. T., Bittman, R. et al. 2002. Structural elucidation of the specificity of the antibacterial agent triclosan for malarial enoyl acyl carrier protein reductase. *J Biol. Chem.*, 277: 13106–13114.
12. Surolia, N., Surolia, A. 2001. Triclosan offers protection against blood stages of malaria by inhibiting enoyl- ACP reductase of Plasmodium falciparum. *Nat Med*, 7: 167–173.
13. Maestrelli, F., Mura, P., Alonso, M. J. 2004. Formulation and characterization of triclosan sub-micron emulsions and anocapsules. *J Microencapsul.*, 21: 857–864.
14. Shailendra, Kumar Sharma., Prasanna, Parasuraman., Gyanendra, Kumar., Namita, Surolia., & Avadhsha, Surolia. 2007. Green Tea Catechins Potentiate Triclosan Binding to Enoyl-ACP Reductase from Plasmodium falciparum (PfENR). *J. Med. Chem.*, 50:765-775.

15. Joel, S. Freundlich., John, W. Anderson., Dimitri, Sarantakis., Hong-Ming, Shieh., Min Yu., Juan-Carlos, Valderramos., Edinson, Lucumi., Mack, Kuo., William, R. Jacobs., Jr. David, A. Fidock., Guy, A. Schiehser., David, P. Jacobus., & James, C. Sacchettini. 2006. Erratum to "Synthesis, biological activity, and X-ray crystal structural analysis of diaryl ether inhibitors of malarial enoyl acyl carrier protein reductase. Part 1: 4'-Substituted triclosan derivatives. *Bioorganic & Medicinal Chemistry Letters*, 16: 3618–3619.
16. Discoverystudio2.5. Accelrys, Inc., SanDiego, CA, 2009, <http://www.accelrys.com>.
17. Smellie, A., Teig, S., Towbin, P. 1994. *J.Comput.Chem.*, 16:171.
18. Brooks, B. R., Brucolleri, R. E., Olafson, B. D., States, D.J., Swaminathan, S., & Karplus, M. J. 1983. *J. Comput. Chem.*, 4:187.
19. Freundlich, J. S., Wang, F., Tsai, H. C., Kuo, M., Shieh, H. M., Anderson, J. W., Nkrumah, L. J., Valderramos, J. C., Yu, M., Kumar, T. R., Valderramos, S. G., Jacobs, W. R. Jr., Schiehser, G. A., Jacobus, D. P., Fidock, D. A., & Sacchettini, J. C. 2007. X-ray structural analysis of Plasmodium falciparum enoyl acyl carrier protein reductase as a pathway toward the optimization of triclosan antimalarial efficacy. *J Biol Chem.*, 282(35):25436-44.
20. Li, H., Sutter, J., & Hoffmann, R. 2000. HypoGen: An Automated System for Generating Predictive 3D Pharmacophore Models., in *Pharmacophore Perception, Development, and use in Drug Design*. O. F. Guner (Ed.), International University Line, La Jolla, CA,.
21. Guner, O. F. 2000. In *Pharmacophore Perception, Development, and Use in Drug Design*; International University Line: La Jolla, California, p173.
22. Wu, G., Robertson, D. H., Brooks, C. L. III, Vieth, M. 2003. Detailed Analysis of Grid-Based Molecular Docking: A Case Study of CDOCKER - A CHARMM-Based MD Docking Algorithm. *J. Comp. Chem.*, 24:1549.
23. Garcia, Linares., Guadalupe, E., & Rodriguez, Juan B. 2007. Current Status and Progresses Made in Malaria Chemotherapy. *Current Medicinal Chemistry*, 14(3):289-314

## Molecules – Training Set-18







Molecules – Test Set-23

